

## Article

# Effects of Injection Parameters and EHN Mixing on the Combustion Characteristics of Fueling Pure Methanol in a Compression Ignition Engine

Haifeng Liu <sup>1</sup>, Mengjia Li <sup>1</sup>, Hongyuan Wei <sup>2</sup>, Can Wang <sup>1</sup>, Tengda Song <sup>1</sup>, Zhixiong Huang <sup>1</sup>, Zhao Zhang <sup>3</sup>, Yanqing Cui <sup>4,5,\*</sup> and Chao Jin <sup>6,\*</sup>

<sup>1</sup> State Key Laboratory of Engines, Tianjin University, Tianjin 300072, China; haifengliu@tju.edu.cn (H.L.); lmjqaq3721@163.com (M.L.); wang\_can@tju.edu.cn (C.W.); 2020201334@tju.edu.cn (T.S.); 2021201160@tju.edu.cn (Z.H.)

<sup>2</sup> China Automobile Technology & Research Center Co., Ltd., Tianjin 300162, China; weihongyuan@catarc.ac.cn

<sup>3</sup> School of Automation, Chengdu University of Information Technology, Chengdu 610225, China; zhangzhao@cuit.edu.cn

<sup>4</sup> Department of Mechanical Engineering, The Hong Kong Polytechnic University, Hong Kong 100872, China

<sup>5</sup> Department of Industrial & Systems Engineering, The Hong Kong Polytechnic University, Hong Kong 100872, China

<sup>6</sup> School of Environmental Science and Engineering, Tianjin University, Tianjin 300072, China

\* Correspondence: yanqingcui@tju.edu.cn (Y.C.); jinchao@tju.edu.cn (C.J.)

**Abstract:** As one of the most ideal alternative fuels for internal combustion engines, methanol can achieve near-zero carbon emissions. The main problem of methanol application in compression combustion engines is the phase lag caused by its poor combustion characteristics, but under low load conditions, the fuel activity can be improved by adding the cetane number improver EHN (Isooctyl nitrate), and the dependence on intake heating can be reduced to a certain extent. Based on a three-dimensional CFD simulation, the effects of methanol injection parameters and the addition of EHN on the combustion characteristics of a four-stroke exhaust turbocharged diesel engine were studied in this paper. With or without EHN, the increase in injection pressure and the advance in injection timing lead to an increase in the peak temperature, pressure, and heat release rate, as well as a shortening of the combustion duration. Adding EHN witnesses reduced requirements for methanol ignition, including a decreased peak temperature, pressure, and heat release rate, a significantly shortened ignition delay period, and an extended combustion duration, which thus results in a reduced indicated thermal efficiency. This study innovatively develops a 3D model of a compression combustion engine applicable to in-cylinder direct injection pure methanol fuel and EHN under small load conditions, which provides a reference for future research and development of small-load pure methanol compression combustion engines and has certain guiding significance.

**Keywords:** compression ignition engine; methanol; injection parameters; EHN; numerical simulation



**Citation:** Liu, H.; Li, M.; Wei, H.; Wang, C.; Song, T.; Huang, Z.; Zhang, Z.; Cui, Y.; Jin, C. Effects of Injection Parameters and EHN Mixing on the Combustion Characteristics of Fueling Pure Methanol in a Compression Ignition Engine. *Processes* **2024**, *12*, 48. <https://doi.org/10.3390/pr12010048>

Academic Editor: Blaž Likozar

Received: 30 November 2023

Revised: 20 December 2023

Accepted: 21 December 2023

Published: 24 December 2023



**Copyright:** © 2023 by the authors. Licensee MDPI, Basel, Switzerland. This article is an open access article distributed under the terms and conditions of the Creative Commons Attribution (CC BY) license (<https://creativecommons.org/licenses/by/4.0/>).

## 1. Introduction

With the rapid development of the transportation industry and the continuously increasing demand for engineering power machinery and equipment, the carbon emissions generated by the transportation industry are increasing. However, excessive emissions of carbon dioxide are the main factor that causes greenhouse effects [1–3]. China has introduced relevant carbon reduction policies to reduce carbon dioxide emissions in various industries. The energy revolution, under the guidance of the “Carbon peaking and Carbon neutrality” target, means that it is necessary to transform the traditional energy system dominated by fossil energy into one dominated by renewable energy and complementary energy, thereby promoting the upgrading of China’s energy and related industries.

As one of many alternative fuels, methanol has attracted a lot of attention in recent years with its extensive sources and diverse features [4–8]. Compared with traditional fossil fuels such as diesel or gasoline, methanol only has one carbon atom and a lower C/H ratio, which makes it easier to make and has great potential to reduce carbon dioxide emissions [5]. In addition, methanol has a high octane number and good anti-explosion performance, allowing for the utilization of a high compression ratio to increase thermal efficiency and reduce fuel consumption [7]. The latent heat of evaporation is significantly high, which has the advantages of reducing combustion temperature, heat loss, and NOx emissions [9].

An engine fueled with methanol has good emission characteristics, including ultra-low CO, NOx, HC, PAH, and soot emissions [9]. However, methanol also has some challenges when burned in the engine. For example: (1) The lower cetane number limits the working range of a methanol engine, which usually needs to be ignited by the dual-fuel combustion mode [10]; (2) Cold starting difficulties are caused by lower in-cylinder pressure and combustion temperature; and (3) Tail gas contains higher alcohol, aldehyde, and other unregulated emissions, causing new environmental pollution [11,12]. The challenges of methanol drive the technical renewal of internal combustion engines. On one hand, from the perspective of the fuel structure of China's transportation industry, the consumption of diesel used in the internal combustion engine is much higher than gasoline [1]. The application of methanol to the compression ignition engine has a positive effect on reducing diesel. On the other hand, due to the restriction of throttling loss and compression ratio under spark ignition combustion mode, the thermal efficiency of spark ignition engines is lower [13]. Therefore, compression ignition for methanol has the potential to have more advantages than spark ignition modes, especially for large engines.

The application of methanol fuel to the compression ignition engine mainly has the following three methods: The emulsification method is used to solve the problem of fuel co-solvents through the appropriate emulsifier. The prototype engine can be operated without major modification [14–18]. The methanol/diesel dual-fuel combustion method has two sets of fuel injection systems, with relatively high costs and complicated control. The average substitution rate of methanol to diesel can be achieved by more than 30–90% [19–24], which depends on whether the injection of methanol is direct-injection or port-injection. Direct compression combustion of methanol can be achieved in inlet heating mode, but it is still a great challenge to achieve a high inlet temperature under low load conditions [25–29]. In addition, it can also add a cetane number improver to EHN to improve the auto-ignition reactivity of methanol. Although different improvers have little effect on the cetane number of methanol mixing fuel, there is no doubt that the use of the cetane number improver can reduce the requirements of intake pressure and temperature for stable combustion by changing the ignition temperature and reaction path of the fuel [30–34].

However, at low load, the boundary conditions in engine operation feature lower cylinder temperature and pressure, a smaller amount of fuel injection, and a higher mixture dilution. Especially when methanol is used as fuel, due to its low cetane number and high latent heat of evaporation, it is difficult for methanol compression ignition engines to operate stably without intake heating under low load conditions at low and medium speed, which has been confirmed by previous experiments [35]. Furthermore, intake heating requires external energy. In order to reduce the dependence on intake heating, cetane number improvers can be added to methanol to improve fuel activity.

EHN (Isooctyl nitrate) is a widely used cetane number improver and dominates the market [36]. The chemical formula of EHN is  $C_8H_{17}NO_3$ , and the low calorific value is 27.4 MJ/kg [37]. Adding 0.1% EHN to methanol/biodiesel can increase the cetane number of the fuel by 2~9 [38]. Relevant experimental results show that adding 3% EHN to methanol can improve fuel activity and reduce the dependence on intake heating under low load conditions [35]. At present, studies on the effects of a cetane number improver on the combustion characteristics of a methanol compression ignition engine under low load are very limited [39,40]. MAN Company [41] produced a methanol compression combustion

engine and added a cetane number improver of 5% by volume to the methanol consumed. Cui et al. [42] studied the effect of a cetane number improver on the performance of a direct injection pressure combustion engine. When the cetane number improver is 4%, the engine can be cold-started and have stable operation at ambient temperatures of  $-2.5$  °C. At a coolant temperature of 40 °C, only a 2% cetane number improver is required to achieve a cold start. At low speed and low load, a 3% cetane number improver is used, and the engine speed fluctuates slightly. After using a 4–5% cetane number improver, the specific energy consumption of the methanol compression combustion engine is lower than that of the original diesel engine. Michael et al. [43] also used a mixture of 5% cetane number improver and 95% methanol on compression-combustion engines with different compression ratios. The results show that blended fuel works well in engines with compression ratios of 16.7:1 and 20:1. The 16.7:1 compression ratio can achieve the highest indicated thermal efficiency of 49%, and the 20:1 compression ratio is 52%.

The method of applying a cetane number improver to a methanol compression combustion engine has the advantages of low cost, simple process, obvious effect, and flexibility. However, more experimental studies have been carried out on the application of methanol-added EHN in compression combustion engines at present, but the understanding of combustion mechanisms is still limited. Based on a turbocharged compression ignition engine with in-cylinder direct injection of methanol, the current study innovatively develops a 3D model of a compression combustion engine applicable to in-cylinder direct injection of pure methanol fuel and EHN additive under small load conditions. The model is established by the 3D CFD simulation software CONVERGE, and the chemical reaction mechanism of methanol is coupled with the numerical simulation of a single working condition of the engine. The effects of injection parameters on the combustion process of engines with or without the cetane number additive EHN under small load conditions were analyzed. This study provides a reference for future research and development of small-load pure methanol compression combustion engines and has certain guiding significance.

## 2. Numerical Model Establishment and Validation

### 2.1. Model Setup

The simulation work in this article is based on a four-stroke diesel engine equipped with an exhaust gas turbocharger. It uses a high-pressure common rail system with a maximum fuel injection pressure of 180 MPa. In order to reduce the dependence of methanol compression on the intake heating, the compression ratio of 17.5:1 of the prototype engine was changed to 21.5:1 to improve the temperature and pressure in the cylinder. The main technical parameters of the engine are shown in Table 1. The sensitivity and uncertainty of the main test instruments are detailed in Table 2.

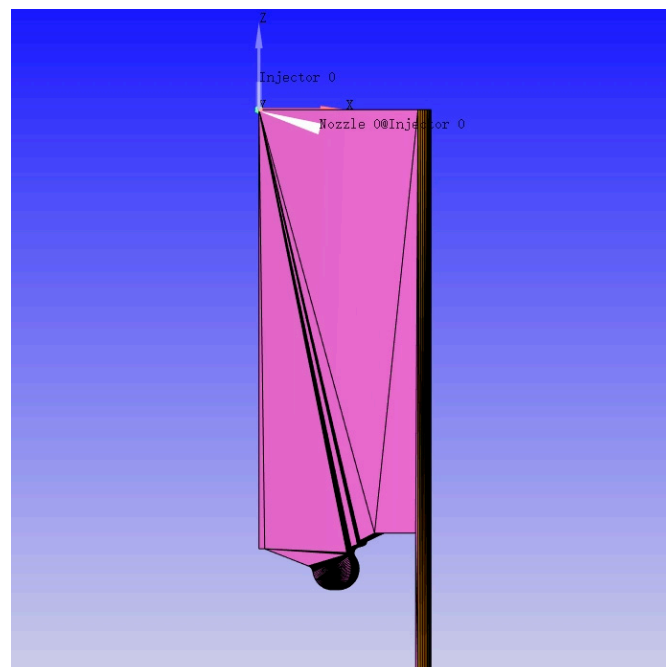
**Table 1.** The main technical parameters of a methanol engine.

Parameter Name (Unit)	Value
Engine	Six cylinders in line, water cooling, four strokes
Displacement (L)	7.7
Bore (mm) × stroke (mm)	110 × 135
Geometric compression ratio	21.5:1
Number of valves per cylinder	4
Theoretical calibration power (kw/rpm)	235/2200
Theoretical maximum torque (N·m/rpm)	1350/(1100–1600)
Number of spray holes	8
Spray hole diameter	0.153
Jet hole angle (°)	147
Booster system	Exhaust gas turbocharger

**Table 2.** Sensitivity and uncertainty of the main test instruments.

Test Parameter	Range	Sensibility	Test Error
Engine torque	0~2100 N·m	±2.8 N·m	±0.2%
Engine speed	0~7000 rpm	±1 rpm	±0.01%
Pressure	0~250 bar	16 pC/bar	±0.4%
Air mass flow	0~2500 kg/h	±1.75 kg/h	±0.5%
Fuel mass flow	0~150 kg/h	±0.01 kg/h	±1%
Intake pressure	0~1000 kPa	±0.5% kPa	±0.1%
Intake Temperature	223.15~573.15 K	±0.05% K	±0.35%

In this study, the combustion chamber model of a diesel engine is established based on Solidworks 2021 software, and the follow-up research is carried out based on CONVERGE software. In order to reduce the calculation workload, the simulation process was selected from 140.5° CA BTDC when the intake valve was closed to 97° CA ATDC when the exhaust valve was opened, so the intake and exhaust structures were not included in the model, as shown in Figure 1. In order to further simplify the calculation, only 1/8 of the total volume of the combustion chamber was generated. The basic mesh size was selected as 2 mm, and mesh encryption was carried out on the injection area, cylinder head, cylinder wall, and piston top near the wall. The encryption series were respectively 2, 2, and 1, and the maximum mesh number was 442,075. The main physical models and chemical models involved are shown in Table 3 [41–43]. For combustion modeling, the SAGE detailed chemical kinetics solver was used with the chemical kinetic mechanism for methanol/EHN developed by Chang et al. [44] to model the methanol/EHN combustion, which contains 61 species and 479 elementary reactions. Table 4 shows the initial environmental parameters, wall boundary parameters, and fuel injection parameters. Parameter 1 is the related parameter of a pure methanol engine. Parameter 2 is the relevant parameter for methanol blending with 3%<sub>v</sub> EHN.

**Figure 1.** CONVERGE combustion chamber 1/8 model.

**Table 3.** Model selection.

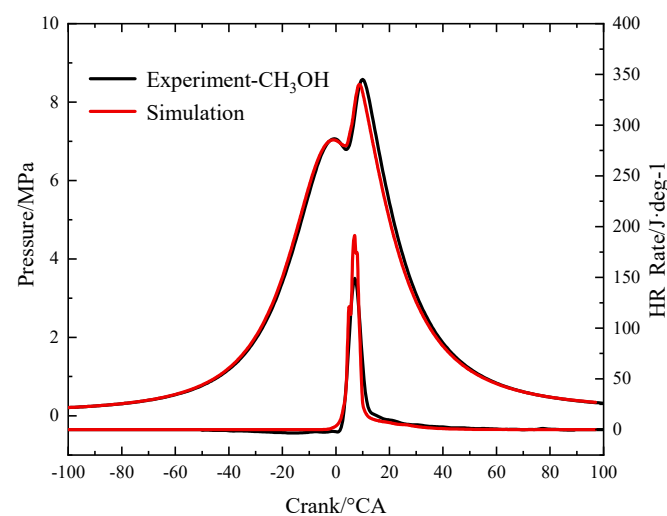
Item	Model
Turbulence flow modeling	RNG $k - \epsilon$
Spray model	KH-RT
Collisional polymerization model	NTC
Droplet collision model	Wall film-O'Rourke
Fuel evaporation model	Frossling
Combustion model	SAGE
Nitrogen oxide generation model	Zeldovich
Carbon smoke generation model	Hiroyasu Soot

**Table 4.** Initial air parameters, wall boundary conditions, and fuel injection parameters.

Item (Unit)	Value	
	Pure Methanol	Methanol + 3% <sub>v</sub> EHN
Intake temperature (K)	394.5	394.5
Intake pressure (MPa)	0.135	0.135
Turbulent kinetic energy ( $m^2/s^2$ )	20.0	20.0
Turbulent dissipation number	17,183.4	17,183.4
Cylinder head temperature (K)	450	450
Wall temperature (K)	450	450
Piston top temperature (K)	500	500
Injection timing ( $^{\circ}$ CA ATDC)	-12	-12
Fuel injection quantity (mg)	49	49
Injection pressure (MPa)	40	25
Injection duration ( $^{\circ}$ CA)	16.7	21.2

## 2.2. Model Validation

In the experiment, the cylinder pressure measurement equipment is a 6125A AVL pressure sensor (Sourced from Liszt Technology Center Co., LTD, Tianjin, China) and a 5011B charge amplifier (Sourced from Xieke Industrial Control Equipment Co., LTD, Shanghai, China) with a sensitivity of  $-16$  pc/bar. The test error is  $\pm 0.4\%$ . The experimental data with a speed of 1200 rpm and a load of 10% are selected for calibration. The simulation results and experiments are compared, as shown in Figures 2 and 3. The comparison error analysis of the simulation calculation and experiment is shown in Table 5. The black line represents the experimental data of the pure methanol engine and the methanol engine after adding 3% volume fraction of EHN, and the red line represents the simulation results. It can be seen that the prediction results match well with the experimental results.

**Figure 2.** Comparison between simulation and experiment results of combustion pressure and heat release rate in a cylinder fueled with methanol.

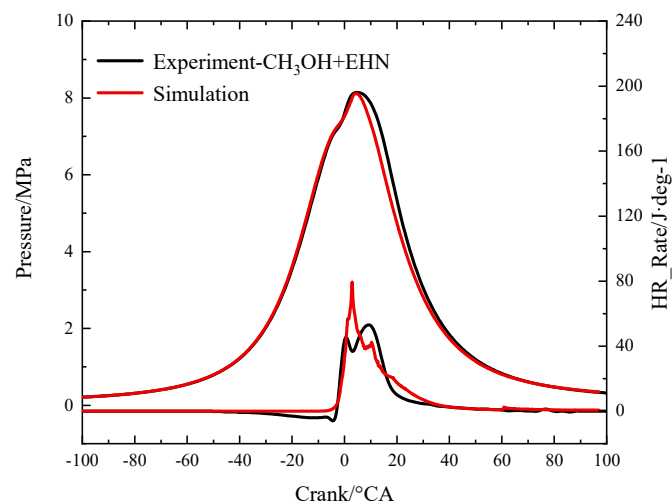


**Figure 3.** Comparison between simulation and experiment results of combustion pressure and heat release rate in cylinders fueled with methanol and 3%<sub>v</sub> EHN.

**Table 5.** Error analysis of the comparison between simulation results and experiments.

Item (Unit)	Experiment	Simulation	Experiment	Simulation
Fuel	Pure Methanol	Pure Methanol	Methanol + 3% <sub>v</sub> EHN	Methanol + 3% <sub>v</sub> EHN
Peak cylinder pressure (MPa)	8.58	8.45	8.14	8.10
Crank angle at peak cylinder pressure (°CA ATDC)	10	8.81	4.5	4.4
Peak heat release rate (J)	149.127	191.34	53.13	79.45
Crank angle at peak heat release rate (°CA ATDC)	7	7	9	3.0
Total heat release (J)	942.12	1008.32	1033.14	966.12
CA10 (°CA ATDC)	5	4.4	3	1.4
CA50 (°CA ATDC)	8	7.11	10.5	9.6
CA90 (°CA ATDC)	25.5	16.1	27	29.6
NO <sub>x</sub> (g/kW·h)	12.69	14.44	5.67	6.25

### 3. Results and Discussions

#### 3.1. The Influence of Fuel Injection Pressure and EHN Addition on Combustion Characteristics

Because the low heating value of methanol is lower than that of diesel [40], which is only 19.93 MJ/kg. To ensure the same heat input, more methanol needs to be injected. However, under the same injection pressure, the injection duration will be extended, which is not conducive to the indicated thermal efficiency. Therefore, in this article, different injection pressures are investigated to shorten the injection duration of methanol. The improvement of fuel injection pressure has a direct impact on the formation of mixtures in the cylinder, which will then affect the combustion efficiency of the engine and emissions. The five different fuel injection pressures of 25 MPa, 30 MPa, 35 MPa, 40 MPa, and 50 MPa through verified models in this section are modified to explore the effects of different fuel injection pressures on the combustion characteristics of methanol engines under low load conditions. Combined with EHN addition, the effects of fuel injection pressure on combustion characteristics are further studied under the same engine operation conditions.

### 3.1.1. The Effect of Fuel Injection Pressure on Temperature

According to the mechanism, the effect of adding EHN on pure methanol combustion is reflected in reducing the temperature required for ignition. Therefore, the temperature in the engine cylinder will be analyzed below. As shown in Figure 4, the in-cylinder temperature increases with the increase in fuel injection pressure, but the maximum in-cylinder temperature of pure methanol is higher than that after adding EHN. The maximum average temperature in the cylinder of the pure methanol engine exceeds 1300 K, while the maximum average temperature in the cylinder does not exceed 1200 K after adding EHN under 25 MPa. After adding EHN, the ignition delay period is shortened, the gas temperature in the cylinder rises in advance, the evaporation rate of methanol is accelerated, the quality of the mixed gas distribution in the cylinder is improved, and the formation of the ignition point is conducive to the development of the methanol flame. However, as shown in Figures 5 and 6, after adding EHN, the primitive reactions with the largest temperature sensitivity values changed greatly. For pure methanol combustion, due to a long ignition delay period, methanol starts to burn at a higher temperature, and high-temperature reactions such as  $\text{H}_2\text{O}_2 (+\text{M}) = 2\text{OH} (+\text{M})$  have a higher sensitivity. Reactions related to  $\text{HO}_2$  and  $\text{H}_2\text{O}_2$  have a greater impact on temperature because  $\text{HO}_2$  will participate in the multi-step reaction and account for a high proportion in the total reaction of pure methanol combustion. So the reaction temperature sensitivity associated with  $\text{HO}_2$  is higher. After the addition of EHN, the influence of  $\text{HO}_2$ -related elementary reactions on the temperature of methanol combustion disappears, resulting in the disappearance of the influence of the elementary reactions on promoting temperature growth. This is mainly due to the change in the reaction path of  $\text{HO}_2$  after the addition of EHN. The reaction of  $\text{HO}_2$  with methanol is no longer the main reaction, but the reaction with other components generates an active free radical-promoting reaction. In the  $\text{CH}_3\text{OH} \rightarrow \text{CH}_2\text{OH} \rightarrow \text{CH}_2\text{O} \rightarrow \text{HCO}$  reaction path, the proportion of  $\text{OH}$  and  $\text{NO}_2$  participating in the reaction increases. As a result, the addition of EHN reduces the temperature during the methanol reaction, and the temperature in the cylinder is generally lower than that in the cylinder of pure methanol combustion. In addition to the influence of latent heat of vaporization, with the addition of EHN and the increase in injection pressure, the ignition delay period is shortened, methanol droplets evaporate earlier, and the latent heat of vaporization occurs earlier, which further leads to a lower temperature in the cylinder. thus affecting the improvement of the maximum pressure and peak heat release rate in the cylinder.

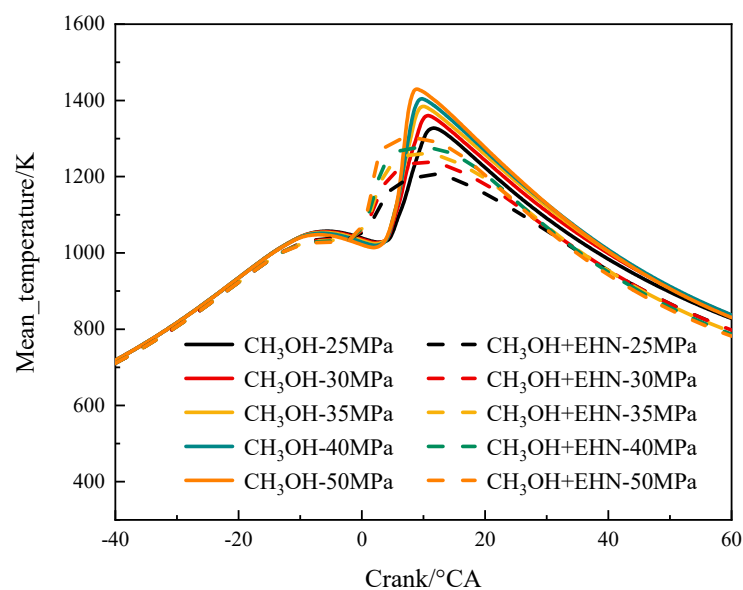


**Figure 4.** Variations in the in-cylinder mean temperature at different fuel injection pressures.

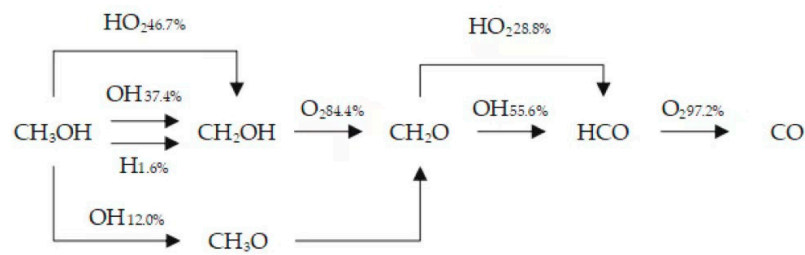


Figure 5. Methanol reaction path with 0%<sub>v</sub> EHN (800 K) [44].

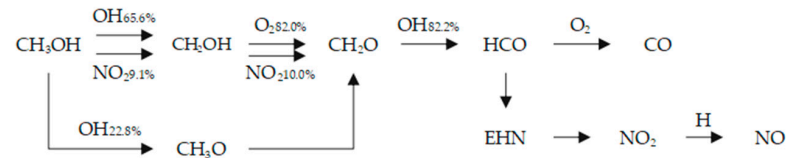


Figure 6. Methanol reaction path with 3%<sub>v</sub> EHN (800 K) [44].

Figure 7 shows the corresponding temperature field distribution at TDC under different injection pressure conditions. It can be observed that the high-temperature region in the cylinder temperature distribution of a pure methanol engine decreases with the increase in injection pressure at TDC. The high-temperature area increases after adding EHN. The reason is that the ignition delay period shortens when adding EHN to methanol. With the increase in fuel injection pressure, the spray breakup condition is improved, which assists in increasing the in-cylinder temperature. Conversely, because pure methanol is not burned at TDC, the most significant impact factor on the temperature in the cylinder is the flow and pressure of the gas in the cylinder. The increase in fuel injection pressure drives the rapid flow of gas in the cylinder, resulting in a decrease in the temperature inside the cylinder. Despite the decrease in high-temperature areas, due to the sufficient mixing of fuel, the burning of fuel is more intense. Therefore, with the improvement of fuel injection pressure, the overall combustion process becomes faster and more concentrated, resulting in an increase in the highest temperature in the cylinder.

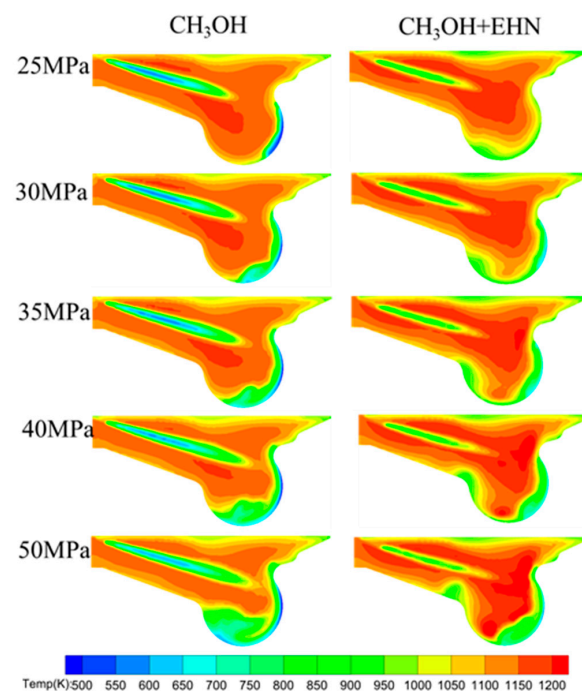
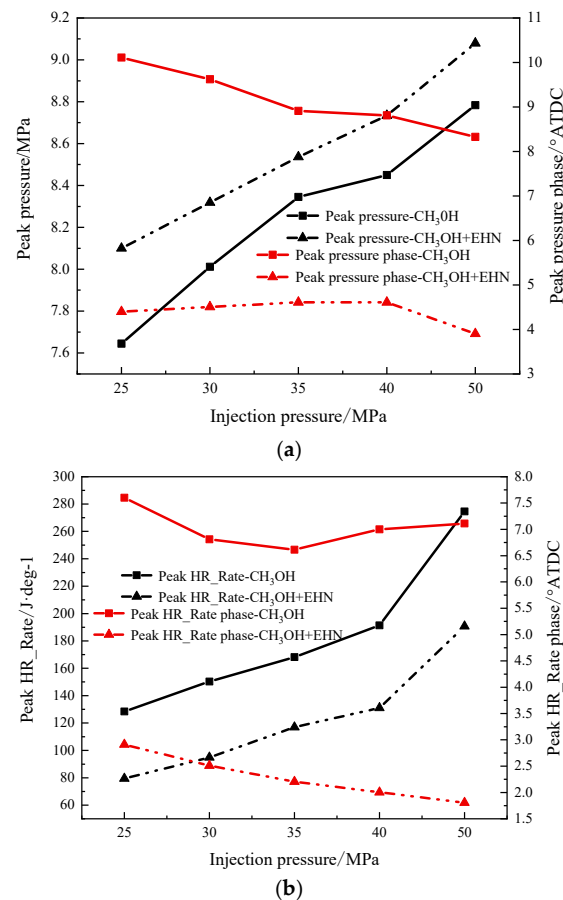


Figure 7. Temperature distribution in the cylinder under different injection pressures at TDC.

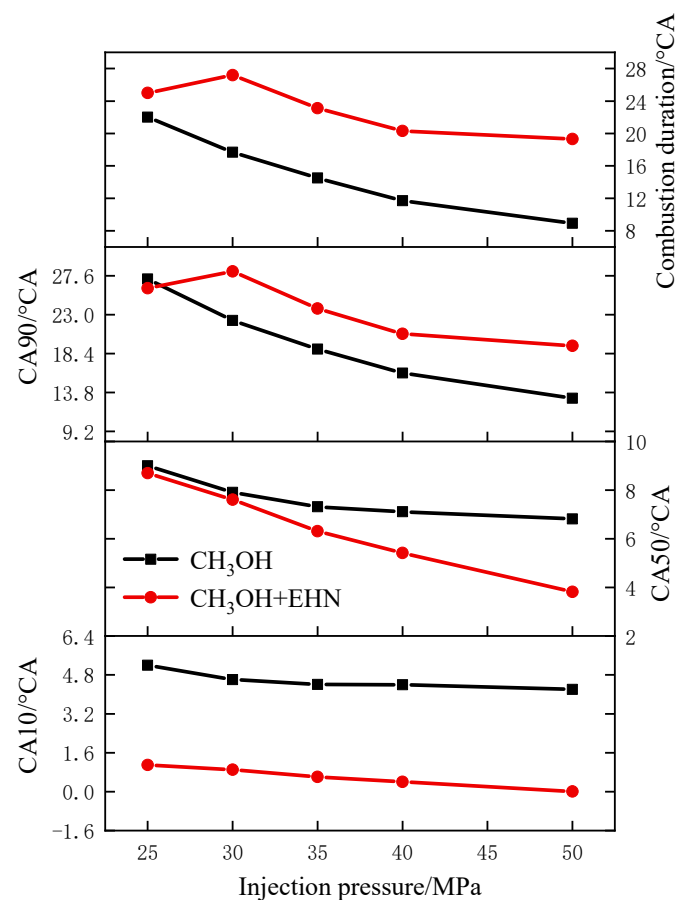
### 3.1.2. The Effect of Fuel Injection Pressure on the Combustion Process

Figure 8 shows the peak pressure and heat release rate in the cylinder under different fuel injection pressures. From Figure 8, it can be found that as the fuel injection pressure increases, with or without EHN, the peaks of in-cylinder pressure and heat release rate of the methanol engine increase accordingly, and the maximum pressure rise rate in the cylinder is basically the same. From the comparison of peak pressure with or without EHN added in Figure 8a, it can be found that with the increase in injection pressure, the peak pressure of a methanol engine increases with or without EHN, while the phase of peak pressure of a pure methanol engine advances. The phase of peak pressure when methanol is added to EHN is delayed from 25 to 40 MPa with the increase in injection pressure and is significantly advanced under the 50 MPa condition. Figure 8b shows the change in the peak heat release rate and the phase of the peak heat release rate. As can be seen from the figure, the peak heat release rate of a methanol engine with or without EHN increases, and the peak phase of the heat release rate advances on the whole, and the change is more regular after adding EHN. It can be seen that the methanol on the combustion chamber wall increases due to the increase in injection pressure, which limits the large increase in in-cylinder pressure. On the whole, the addition of EHN causes an increase in the peak pressure in the cylinder, and the maximum rise is about 0.5 MPa, while the peak heat release rate is significantly reduced, with an average reduction of about 60 J/deg, indicating that the temperature in the cylinder reduces after the addition of EHN. However, when the injection pressure of methanol increases from 35 MPa to 50 MPa after EHN is added, the increase in peak pressure in the cylinder is significant, indicating that the addition of EHN improves the activity of methanol fuel and the probability of stable operation under low speed and low load conditions.



**Figure 8.** Different in-cylinder pressure peaks (a) and the peak of the heat release rate (b) vary with injection pressure variations.

The combustion quality of the mixture in the cylinder is not only affected by the distribution of the concentration of the mixing gas in the cylinder but also by the pressure, temperature, and vortex strength of the cylinder. The ignition delay period is defined as the crank angle between the time of fuel injection and the cumulative heat release rate of 10%. Due to the low pressure and low mixture concentration in the cylinder under low load conditions, the mixture temperature has a greater impact on the ignition delay period. Figure 9 shows the variation trends of CA10, CA50, CA90, and combustion duration under different injection pressures, respectively. It can be concluded that with the increase in injection pressure, the change in ignition delay period is not significant, with or without EHN, while the CA50, or combustion phasing, is significantly advanced and the combustion duration is shortened. By adding EHN, the ignition delay period of methanol combustion is shortened, and the average shortened period is about 4° CA. The CA50 is obviously more advanced than the combustion of pure methanol, and the combustion duration is extended with the addition of EHN.



**Figure 9.** Changes in CA10, CA50, and CA90 under different injection pressures.

According to the mechanism of methanol and EHN, it can be seen that EHN decomposes  $\text{NO}_2$  at low temperatures, which increases the concentration of  $\text{NO}_2$  in the early stage, leading to changes in the reaction path of methanol combustion, promoting the break of the C-H bond in the  $\text{CH}_3\text{OH}$  molecule, and directly promoting the dehydrogenation of methanol. The active free radicals  $\text{C}_7\text{H}_{15-3}$  and  $\text{CH}_2\text{O}$  generated by EHN decomposition also improve the reactivity of the system, promoting the methanol combustion oxidation reaction rate. The combustion oxidation reaction rate is reflected in the burning phenomenon in the cylinder, which promotes the formation of the ignition point. The formation of high-temperature areas in the engine cylinder accelerates, which affects the development and spread of the flame, shortens the ignition delay period, and leads to a concentration of heat release in the cylinder. Adding EHN significantly improves the ignition and cold

start issues of methanol. With the increase in fuel injection pressure, the ignition delay period is shortened slightly, and CA10 is advanced slightly. The reason is that the increase in injection pressure improves the mixing effect of spray diffusion. It can be seen that the degree of shortening the ignition delay period after adding EHN does not have a significant difference with the change in injection pressure, so the injection pressure has a great influence on the exothermic law of methanol but little influence on the exothermic time of methanol.

### 3.1.3. The Effects of Fuel Injection Pressure and EHN on Indicated Thermal Efficiency

As shown in Figure 10, with the improvement of fuel injection pressure, the indicated thermal efficiency (ITE) of a pure methanol engine has also increased, and the ITE is 35.4%, 37.1%, 38.1%, 38.5%, and 38.6%, with injection pressure increasing from 25 MPa to 50 MPa, respectively. After the addition of EHN, the ITE is 34.4%, 34.7%, 35.2%, 35.6%, and 35.3%, respectively. It can be clearly seen from the figure that the increase in indicated thermal efficiency after adding EHN is significantly smaller than that of a pure methanol engine. With the increase in fuel injection pressure, the atomization effect of methanol fuel in the cylinder has improved, and the time of combustion has advanced. As a result, the ITE has also improved with the improvement of the fuel injection pressure. However, the indicated thermal efficiency gap between a pure methanol engine and a methanol-EHN engine widens at high injection pressure conditions. On one hand, the high reactivity additive of EHN ignites a methanol spray flame, which makes the combustion process dominated by mixing-controlled combustion and driven by the methanol injection rate. As a result, the combustion reaction rate slows down and the combustion duration prolongs, which causes the lower indicated thermal efficiency. Instead, when pure methanol is injected, the longer ignition delay caused by its low reactivity may enhance the homogeneity of the combustible charge. The subsequent combustion process is more controlled by the chemical reaction rate, indicating a relatively constant volume of combustion. Therefore, the combustion duration shortens, and the indicated thermal efficiency increases. On the other hand, as fuel injection pressure increases, the indicated thermal efficiency increases because high injection pressure improves the spray breakup condition and increases the combustible mixture inside the cylinder, resulting in CA50 towards TDC.

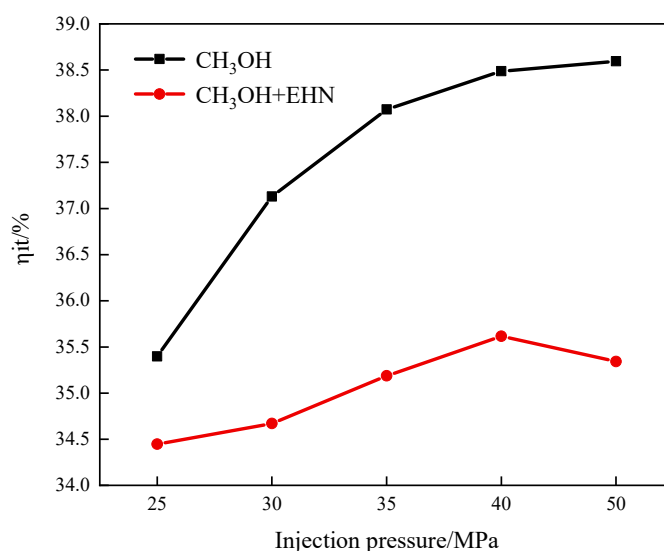


**Figure 10.** Variation of the indicated thermal efficiency at different fuel injection pressures.

### 3.2. The Influence of Fuel Injection Timing and EHN on Combustion

The effect of injection timing on the combustion of a methanol engine cannot be ignored. Too early injection will lead to more homogeneous charge and thus a very high combustion rate, and too late injection will lead to too low temperature in the cylinder

and poor fuel atomization mixing, which cannot be compressed combustion. Therefore, the proper injection timing makes it enter at the best time, which can improve the mixture uniformity and regulate the ignition delay to achieve a stable combustion process. Optimizing injection timing can improve combustion efficiency and reduce fuel consumption and emissions. However, the optimal injection timing varies depending on engine type, fuel characteristics, and operating conditions. Methanol fuel has a long ignition delay period, its cetane number is low, and the spontaneous combustion temperature is high. Injection timings of  $-8^\circ$  CA ATDC,  $-10^\circ$  CA ATDC,  $-12^\circ$  CA ATDC,  $-14^\circ$  CA TDC, and  $-16^\circ$  CA ATDC are selected, and injection pressure is fixed at 40 MPa.

### 3.2.1. The Effect of Fuel Injection Timing and EHN on Temperature

Figure 11 shows the change in the average temperature in the cylinder at different injection timings. It can be obtained with advance injection timing, regardless of whether there is an additional EHN. The average temperature in the cylinder rises, and the maximum temperature in the cylinder also increases with the fuel injection timing advancing. The peak average temperature in the cylinder and the temperature in the cylinder at the later stage of combustion after adding EHN are significantly lower than those of the engine with pure methanol. The reason for this phenomenon is that after the addition of EHN, the primitive reaction with the largest temperature sensitivity value has changed greatly, and the high temperature reaction with high sensitivity and related to  $\text{HO}_2$  has no promoting effect on temperature growth, resulting in the disappearance of the influence of the missing elementary reaction on promoting temperature growth. This is mainly because the reaction path of  $\text{HO}_2$  changes. The reaction of  $\text{HO}_2$  with methanol is no longer the main reaction, but the reaction with other reactant components generates an active free radical-promoting reaction.

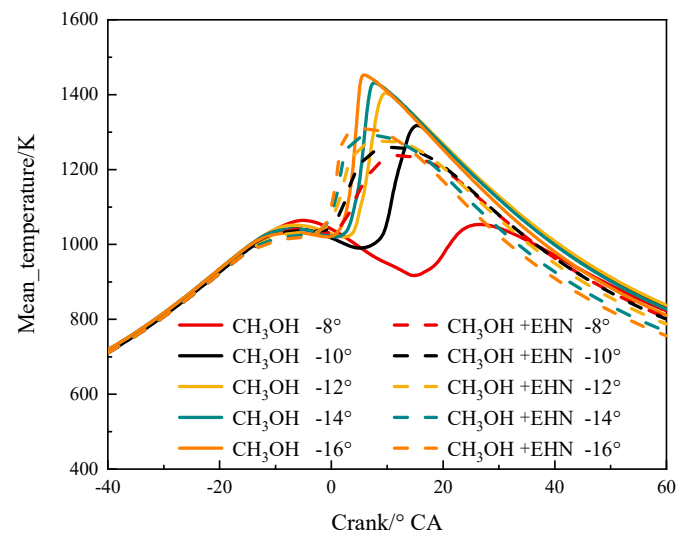


**Figure 11.** Variations in in-cylinder mean temperature at different fuel injection timings.

Figure 12 shows the temperature field distribution at TDC at different fuel injection timings. It can be observed that the high-temperature region of the pure methanol engine at TDC decreases with the advance of fuel injection timing. After adding EHN, the high-temperature area of the temperature distribution in the cylinder increases with the advance of the injection timing. Because of the advance in fuel injection timing, the combustion starting point of methanol mixing with EHN is moving towards TDC, resulting in an increase in the temperature in the cylinder. However, the mixture of pure methanol engines is not compressed ignition near TDC with the advance of injection timing, so the advance of injection timing means that the fuel starts to burn earlier in the process of compression combustion, which leads to the early stage of fuel combustion occurring of the piston close to TDC. Due to the advanced injection timing, the high-temperature region generated by the combustion has spread towards the piston movement before the TDC. In addition, there is a

high latent heat of vaporization and an endothermic phenomenon when more methanol is injected during the ignition delay period, which leads to a decrease in the high-temperature region in the cylinder at the TDC. Despite the decrease in high-temperature areas, due to the sufficient mixed fuel in the ignition delay period, the burning of fuel is more intense. Therefore, with the advance of injection timing, the overall combustion process becomes faster and more concentrated, causing the temperature peak inside the cylinder to rise.

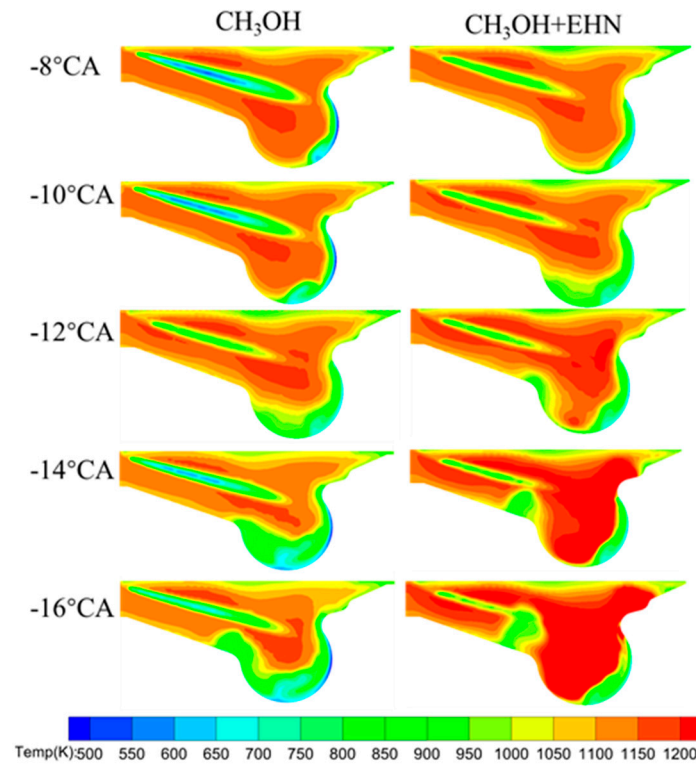


**Figure 12.** Temperature distribution in the cylinder under different injection timings at TDC.

### 3.2.2. The Impact of Fuel Injection Timing and EHN on the Combustion Process

Figure 13 shows the comparison of the peaks of in-cylinder pressure and heat release rate of pure methanol fuel and methanol fuel mixed with EHN at different injection timings. It can be found that as fuel injection timing advances, the peak of cylinder pressure and heat release rate of the methanol engine increase with or without EHN. Compared with the methanol mixing with EHN, the peak pressure and heat release rate of the pure methanol fuel engine increase more greatly. Compared with the increase in EHN addition, the increase in the peak pressure of pure methanol is larger. The peak phase of a pure methanol engine lags behind that of methanol with EHN, and the difference is  $5.76^\circ$  at  $-10^\circ$  ATDC. With the advance of injection timing and the addition of EHN, the peak of heat release rate increases at  $-8^\circ$  ATDC and  $-10^\circ$  ATDC but decreases at  $-12^\circ$  ATDC to  $-16^\circ$  ATDC. This is mainly because under the same amount of fuel injection, the injection timing is advanced, the ignition delay period is extended to form more flammable mixed gas, and the combustion phasing is advanced. When the mixture is ignited, a large amount of mixture formed in the cylinder burns in a very short time, resulting in an increase in the pressure rise rate, the maximum pressure in the cylinder, and the instantaneous heat release rate. Combined with the changing trend of the cylinder pressure curve at injection timing of  $-10^\circ$  CA, it can be seen that the combustion phasing of the methanol under this injection timing is obviously lagging behind. After adding EHN, the peak of the cylinder at injection timing of  $-10^\circ$  CA increases by about 1.26 MPa, and the peak of the heat release rate is significantly reduced by about 45 J/CA, indicating that the temperature in the cylinder after the addition of EHN has decreased, and the thresholds for the fuel to reach the ignition temperature and spontaneous combustion temperature are reduced. The methanol can

spontaneously ignite at a lower temperature after adding EHN. When EHN is mixed with methanol, the variations of the peak of in-cylinder pressure increase more evenly with the injection timing advancing from  $-10^{\circ}$  CA to  $-16^{\circ}$  CA.

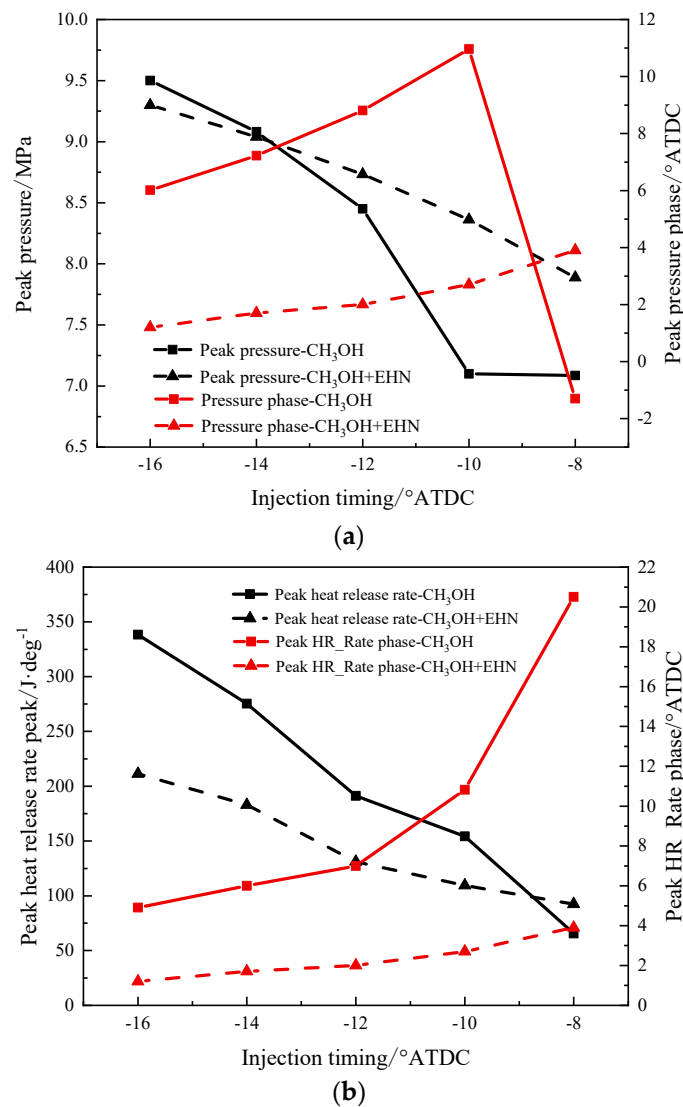


**Figure 13.** Different in-cylinder pressure peaks (a) and the peak of the heat release rate (b) vary with injection timing variations.

Figure 14 shows CA10, CA50, CA90, and combustion duration under different fuel injection pressures. It can be found that with the advance of injection timing, the ignition delay period of a pure methanol engine is shortened first and then extended, which is  $20.7^{\circ}$  CA,  $17.5^{\circ}$  CA,  $16.4^{\circ}$  CA,  $17.3^{\circ}$  CA, and  $18.5^{\circ}$  CA, respectively. The CA10 of a pure methanol engine is significantly advanced, and the CA50, or combustion phasing, also has an obvious advance. After the addition of EHN, the CA10 and CA50 are advanced compared with pure methanol, and the gap between them is also reduced with the advance of injection timing. The CA90 has a delay compared with pure methanol. The combustion duration of pure methanol decreased slightly when EHN was added, from  $-10^{\circ}$  CA to  $-16^{\circ}$  CA, while the combustion duration of pure methanol was significantly extended at  $-8^{\circ}$  CA. With the advance of the injection timing, the flammable mixture of methanol during the ignition delay period increases, and the amount of methanol participating in premixed combustion increases. Under certain temperatures and pressures, the methanol concentration in the cylinder meets the ignition conditions, making the combustion heat release advance and the ignition delay period shorten. However, when the injection time is advanced to  $-14^{\circ}$

CA, the methanol mixture concentration in the cylinder and the temperature and pressure in the cylinder are no longer the best ignition conditions, so the ignition delay period is extended. Because  $\text{NO}_2$  produced by methanol decomposition after adding EHN promoted the C-H bond break of  $\text{CH}_3\text{OH}$ , promoted the methanol combustion oxidation reaction rate, and shortened the combustion delay period, the average shortened period is about  $4^\circ$  CA. The CA50 is also moved forward compared to the combustion of pure methanol, and the combustion duration is significantly extended. When the injection timing is advanced to  $-16^\circ$  CA, the combustion process is more difficult to move forward, and the influence of injection timing on the ignition delay period is small.

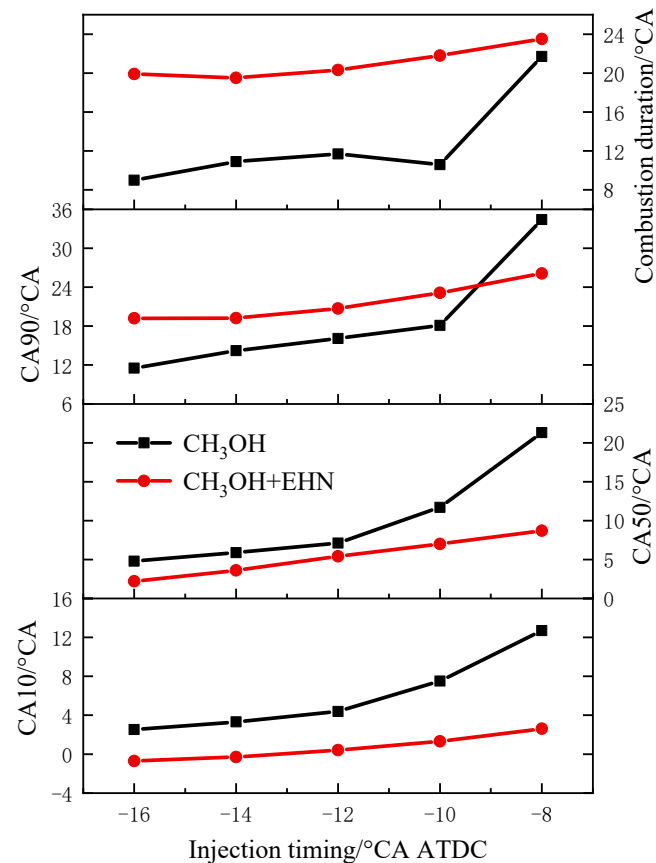


**Figure 14.** Changes in CA10, CA50, and CA90 under different injection timings.

### 3.2.3. The Effects of Fuel Injection Timing and EHN on Indicated Thermal Efficiency

From Figure 15, it can be seen that as the injection timing advances, the indicated thermal efficiency of a pure methanol engine has a trend of rising first and then declining. The highest indicated thermal efficiency is 38.4% at an injection timing of  $-12^\circ$  CA ATDC. The indicated thermal efficiency under other working conditions is 23.3%, 36.2%, 38.3%, and 37.7%, respectively. On one hand, the advance of injection timing makes the combustion phasing advance, and the main combustion occurs near the TDC, which is conducive to the improvement of combustion efficiency. On the other hand, too long ignition delay at early injection timing conditions may cause the over-mixing phenomenon of an air-fuel mixture, which is not good for the formation of combustible gas and hence reduces the efficiency of combustion. When the injection timing is advanced from  $-10^\circ$  CA to  $-12^\circ$  CA, the combustion temperature increases, which plays the main role. After the addition of EHN, the ITE is reduced at injection timings of  $-16^\circ$  CA,  $-14^\circ$  CA,  $-12^\circ$  CA, and  $-10^\circ$  CA, which is 31.6%, 33.1%, 35.6%, and 36.1%, respectively. The reason is that when EHN is mixed with methanol, the ignition delay period is shortened, the evaporation time of methanol droplets is advanced, the heat loss of evaporation latent heat is reduced, and the temperature in the cylinder decreases, leading to a longer combustion duration after adding

EHN, but the combustion efficiency of methanol is reduced. As a result, the indicated thermal efficiency is lower than that of a pure methanol engine. However, pure methanol is difficult to produce in stable and efficient combustion at an injection timing of  $-8^\circ$  CA, which shows an obvious delay in CA10, CA50, and CA90, as mentioned in Figure 14. When blending methanol with EHN, the combustion characteristics have been improved, and hence the indicated thermal efficiency is high.

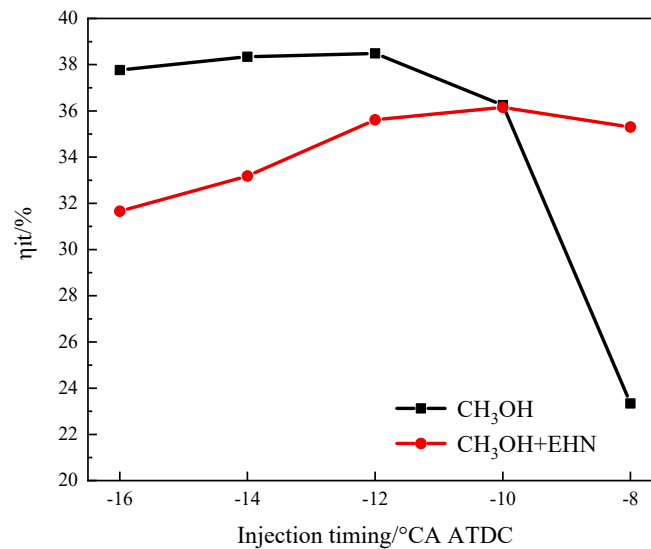


**Figure 15.** Variation of the indicated thermal efficiency at different injection timings.

#### 4. Conclusions

The effects of injection parameters and EHN addition on combustion and emission characteristics of methanol compression ignition engines were investigated in this study based on three-dimensional numerical modeling. The main conclusions are as follows:

- (1) After adding EHN, the ignition condition requirement of methanol is reduced, the ignition delay period is shortened, and the shortening effect of EHN on the combustion delay period is more significant at low temperatures than at high temperatures. The peak temperature in the cylinder decreases, the high temperature region of the temperature distribution in the cylinder at the top dead center increases, the peak pressure in the cylinder and the instantaneous heat release rate decrease, and the combustion duration is extended, which indicates a decrease in thermal efficiency. This is because  $\text{NO}_2$  produced by EHN decomposition can directly promote the dehydrogenation of methanol, and the active free radicals  $\text{C}_7\text{H}_{15-3}$  and  $\text{CH}_2\text{O}$  produced by EHN decomposition also improve the reaction rate. When pure methanol is burned, the temperature at which methanol starts to burn is higher due to the long ignition delay period, and the sensitivity of high-temperature reactions such as  $\text{H}_2\text{O}_2 (+\text{M}) = 2\text{OH} (+\text{M})$  is higher. After adding EHN, the temperature of the methanol reaction is reduced, and the sensitivity of some high-temperature reactions becomes smaller. At the same time, the sensitivity of reactions related to EHN decomposition and early reactions involving decomposition products increased. In the  $\text{CH}_3\text{OH} \rightarrow \text{CH}_2\text{OH} \rightarrow \text{CH}_2\text{O} \rightarrow \text{HCO}$  reaction path, the proportion of OH and  $\text{NO}_2$  participating in the reaction increases.
- (2) The increase in injection pressure can improve the combustion condition of the in-cylinder mixture, resulting in an increase in the peak in-cylinder temperature and an advanced crankshaft angle to reach the peak. The temperature distribution in the cylinder decreases in the corresponding high-temperature region at the TDC. The peak pressure and heat release rate in the cylinder increase with the increase in injection pressure. The variation of the CA10 is not obvious, while the CA50 and CA90 are advanced, and the combustion duration is shortened, indicating an increase in the indicated thermal efficiency.

- (3) The advance of injection timing can make the starting point of combustion near the TDC, and the peak average temperature in the cylinder increases with the advance of the injection timing, and the corresponding crankshaft angle to reach the peak value advances accordingly. The temperature distribution in the cylinder decreases in the corresponding high-temperature region at the TDC. The peak pressure and heat release rate in the cylinder increase with the advance of injection timing. The CA10, CA50, and CA90 are advanced, the combustion duration is shortened, and the thermal efficiency is improved.
- (4) In summary, the addition of EHN resulted in a decrease in the ignition conditions and the temperature in the cylinder. Combined with the change in injection time and injection pressure after adding EHN, it can be seen that the indicated thermal efficiency performance of a pure methanol engine is the best under the conditions of an injection pressure of 40 MPa and an injection time of  $-12^\circ$ . After adding EHN, the indicated thermal efficiency is best when the injection pressure is 40 MPa and the injection time is  $-10^\circ$ . Too high injection pressure or too early injection time will lead to a decrease in its indicated thermal efficiency or no obvious improvement.

**Author Contributions:** Conceptualization, C.W. and M.L.; methodology, C.W. and H.L.; validation, C.W. and M.L.; formal analysis, M.L. and Z.Z.; investigation, Z.H. and M.L.; resources, T.S. and H.W.; data curation, C.W.; writing—original draft preparation, M.L. and Y.C.; writing—review and editing, M.L.; visualization, M.L.; supervision, H.L. and C.J.; project administration, H.L. and C.J.; funding acquisition, H.L. All authors have read and agreed to the published version of the manuscript.

**Funding:** This research was funded by the National Natural Science Foundation of China through Projects 52176125 and U2241262 by Haifeng Liu.

**Data Availability Statement:** Data are contained within the article.

**Conflicts of Interest:** Author Hongyuan Wei was employed by the company China Automobile Technology & Research Center Co., Ltd. The remaining authors declare that the research was conducted in the absence of any commercial or financial relationships that could be construed as a potential conflict of interest.

## References

1. Bae, C.; Kim, J. Alternative fuels for internal combustion engines. *Proc. Combust. Inst.* **2017**, *36*, 3389–3413. [[CrossRef](#)]
2. Dong, S.J.; Cheng, X.B.; Ou, B.; Liu, T.; Wang, Z. Experimental and numerical investigations on the cyclic variability of an ethanol/diesel dual-fuel engine. *Fuel* **2016**, *186*, 665–673. [[CrossRef](#)]
3. Kalghatgi, G.T. Developments in internal combustion engines and implications for combustion science and future transport fuels. *Proc. Combust. Inst.* **2015**, *35*, 101–115. [[CrossRef](#)]
4. Kalghatgi, G.T. Is it really the end of internal combustion engines and petroleum in transport? *Appl. Energy* **2018**, *225*, 965–974. [[CrossRef](#)]
5. Conti, J.; Holtberg, P.; Diefenderfer, J.; LaRose, A.; Turnure, J.T.; Westfall, L. *International Energy Outlook 2016 with Projections to 2040*; United States Energy Information Administration: Washington, DC, USA, 2016.
6. BP. *BP Statistical Review of World Energy 2019*; BP p.l.c.: London, UK, 2019.
7. Yamada, H.; Hayashi, R.; Tonokura, K. Simultaneous measurements of on-road/in-vehicle nanoparticles and NO<sub>x</sub> while driving: Actual situations, passenger exposure and secondary formations. *Sci. Total Environ.* **2016**, *563–564*, 944–955. [[CrossRef](#)] [[PubMed](#)]
8. Wang, Y.H.; Zheng, R.; Qin, Y.H.; Peng, J.; Li, M.; Lei, J.; Wu, Y.; Hu, M.; Shuai, S. The impact of fuel compositions on the particulate emissions of direct injection gasoline engine. *Fuel* **2016**, *166*, 543–552.
9. Abdellatif, T.M.M.; Ershov, M.; Kapustin, V.; Abdelkareem, M.; Kamil, M.; Olabi, A. Recent trends for introducing promising fuel components to enhance the anti-knock quality of gasoline: A systematic review. *Fuel* **2021**, *291*, 120112. [[CrossRef](#)]
10. Goyal, H.; Kook, S.; Lkeda, Y. The influence of fuel ignition quality and first injection proportion on gasoline compression ignition (GCI) combustion in a small-bore engine. *Fuel* **2019**, *235*, 1207–1215. [[CrossRef](#)]
11. Liu, J.; Gong, C.; Peng, L.; Liu, F.; Yu, X.; Li, Y. Numerical study of formaldehyde and unburned methanol emissions of direct injection spark ignition methanol engine under cold start and steady state operating conditions. *Fuel* **2017**, *202*, 405–413. [[CrossRef](#)]
12. Gong, C.; Li, J.; Peng, L.; Chen, Y.; Liu, Z.; Wei, F.; Liu, F. Numerical investigation of intake oxygen enrichment effects on radicals, combustion and unregulated emissions during cold start in a DISI methanol engine. *Fuel* **2019**, *253*, 1406–1413. [[CrossRef](#)]
13. Liu, H.F.; Wang, X.C.; Zhang, D.P.; Dong, F.; Liu, X.; Yang, Y.; Huang, H.; Wang, Y.; Wang, Q.; Zheng, Z. Investigation on Blending Effects of Gasoline Fuel with N-Butanol, DMF, and Ethanol on the Fuel Consumption and Harmful Emissions in a GDI Vehicle. *Energies* **2019**, *12*, 1845. [[CrossRef](#)]

14. Wen, M.S.; Zhang, C.Q.; Yue, Z.Y.; Liu, X.; Yang, Y.; Dong, F.; Liu, H. Effects of Gasoline Octane Number on Fuel Consumption and Emissions in Two Vehicles Equipped with GDI and PFI Spark-Ignition Engine. *J. Energy Eng.* **2020**, *146*, 04020069. [[CrossRef](#)]
15. Alexander, P.; Cristina, I.; Annik, V.B. An effective force field to reproduce the solubility of MTBE in water. *Fuel* **2020**, *264*, 116761.
16. Yang, Q.Y.; Shao, S.; Zhang, Y.; Hou, H.; Qin, C.; Sun, D.; Liu, Y. Comparative study on life cycle assessment of gasoline with methyl tertiary-butyl ether and ethanol as additives. *Sci. Total Environ.* **2020**, *724*, 138130. [[CrossRef](#)] [[PubMed](#)]
17. Pouloupoulos, S.; Philippopoulos, C. Influence of MTBE addition into gasoline on automotive exhaust emissions. *Atmos. Environ.* **2000**, *34*, 4781–4786. [[CrossRef](#)]
18. Franklin, P.; Koshland, C.; Lucas, D.; Sawyer, R.F. Evaluation of combustion by-products of MTBE as a component of reformulated gasoline. *Chemosphere* **2001**, *42*, 861–872. [[CrossRef](#)] [[PubMed](#)]
19. Facetti, J.F.; Nunez, R.; Gomez, C.; Ojeda, J.; Bernal, C.; Leon-Ovelar, R.; Carvallo, F. Methyl tert-butyl ether (MtBE) in deep wells of the Patiño Aquifer, Paraguay: A preliminary characterization. *Sci. Total Environ.* **2019**, *647*, 1640–1650. [[CrossRef](#)]
20. Rosell, M.; Lacorte, S.; Barceló, D. Simultaneous determination of methyl tert-butyl ether, its degradation products and other gasoline additives in soil samples by closed-system purge-and-trap gas chromatography–mass spectrometry. *J. Chromatogr. A* **2006**, *1132*, 28–38. [[CrossRef](#)]
21. Geo, V.E.; Godwin, D.J.; Thiagarajana, S.; Saravanan, C.; Aloui, F. Effect of higher and lower order alcohol blending with gasoline on performance, emission and combustion characteristics of SI engine. *Fuel* **2019**, *256*, 115806.
22. Wang, C.M.; Li, Y.F.; Xu, C.S.; Badawy, T.; Sahu, A.; Jiang, C. Methanol as an octane booster for gasoline fuels. *Fuel* **2019**, *248*, 76–84. [[CrossRef](#)]
23. Waluyo, B.; Setiyo, M.; Saifudin; Wardana, I. Fuel performance for stable homogeneous gasoline-methanol-ethanol blends. *Fuel* **2021**, *294*, 120565. [[CrossRef](#)]
24. Bilgin, A.; Sezer, I. Effects of methanol addition to gasoline on the performance and fuel cost of a spark ignition engine. *Energy Fuels* **2008**, *22*, 131–142. [[CrossRef](#)]
25. Abu-Zaid, M.; Badran, O.; Yamin, J. Effect of Methanol Addition on the Performance of Spark Ignition Engines. *Energy Fuels* **2004**, *18*, 312–315. [[CrossRef](#)]
26. Hao, H.; Liu, Z.W.; Zhao, F.Q.; Du, J.; Chen, Y. Coal-derived alternative fuels for vehicle use in China: A review. *J. Clean. Prod.* **2017**, *141*, 774–790. [[CrossRef](#)]
27. Karavalakis, G.; Short, D.; Vu, D.; Russell, R.L.; Asa-Awuku, A.; Jung, H.; Johnson, K.C.; Durbin, T.D. The impact of ethanol and iso-butanol blends on gaseous and particulate emissions from two passenger cars equipped with spray-guided and wall-guided direct injection SI (spark ignition) engines. *Energy* **2015**, *82*, 168–179. [[CrossRef](#)]
28. Liu, Z.; Sun, P.; Du, Y.D.; Yu, X.; Dong, W.; Zhou, J. Improvement of combustion and emission by combined combustion of ethanol premix and gasoline direct injection in SI engine. *Fuel* **2021**, *292*, 120403. [[CrossRef](#)]
29. Silva, A.; Hauber, J.; Cancino, L.R.; Huber, K. The research octane numbers of ethanol-containing gasoline surrogates. *Fuel* **2019**, *243*, 306–313. [[CrossRef](#)]
30. Zhuang, Y.; Ma, Y.F.; Qian, Y.J.; Teng, Q.; Wang, C. Effects of ethanol injection strategies on mixture formation and combustion process in an ethanol direct injection (EDI) plus gasoline port injection (GPI) spark-ignition engine. *Fuel* **2020**, *268*, 117346. [[CrossRef](#)]
31. Park, C.; Choi, Y.; Kim, C.; Oh, S.; Lim, G.; Moriyoshi, Y. Performance and exhaust emission characteristics of a spark ignition engine using ethanol and ethanol-reformed gas. *Fuel* **2010**, *89*, 2118–2125. [[CrossRef](#)]
32. Turner, D.; Xu, H.; Cracknell, R.F.; Natarajan, V.; Chen, X. Combustion performance of bio-ethanol at various blend ratios in a gasoline direct injection engine. *Fuel* **2011**, *90*, 1999–2006. [[CrossRef](#)]
33. Ceviz, M.A.; Yüksel, F. Effects of ethanol–unleaded gasoline blends on cyclic variability and emissions in an SI engine. *Appl. Therm. Eng.* **2005**, *25*, 917–925. [[CrossRef](#)]
34. He, B.Q.; Wang, J.X.; Hao, J.M.; Yan, X.G.; Xiao, J.H. A study on emission characteristics of an EFI engine with ethanol blended gasoline fuels. *Atmos. Environ.* **2003**, *37*, 949–957. [[CrossRef](#)]
35. Balki, M.K.; Sayin, C.; Canakci, M. The effect of different alcohol fuels on the performance, emission and combustion characteristics of a gasoline engine. *Fuel* **2014**, *115*, 901–906. [[CrossRef](#)]
36. Esan, A.O.; Adeyemi, A.D.; Ganesan, S. A review on the recent application of dimethyl carbonate in sustainable biodiesel production. *J. Clean. Prod.* **2020**, *257*, 120561. [[CrossRef](#)]
37. Kartikeya, S.; Vimal, C.S. Synthesis of organic carbonates from alcoholysis of urea: A review. *Catal. Rev.* **2017**, *59*, 1–43.
38. Maier, T.; Härtl, H.; Jacob, E.; Wachtmeister, G. Dimethyl carbonate (DMC) and Methyl Formate (MeFo): Emission characteristics of novel, clean and potentially CO<sub>2</sub>-neutral fuels including PMP and sub-23 nm nanoparticle-emission characteristics on a spark-ignition DI-engine. *Fuel* **2019**, *256*, 115925. [[CrossRef](#)]
39. Labeckas, G.; Slavinskas, S.; Vilutiene, V. Effect of the cetane number improving additive on combustion, performance, and emissions of a DI diesel engine operating on JP-8 fuel. *J. Energy Eng.* **2015**, *141*, C4014005. [[CrossRef](#)]
40. Lü, X.; Yang, J.; Zhang, W.; Huang, Z. Improving the combustion and emissions of direct injection compression ignition engines using oxygenated fuel additives combined with a cetane number improver. *Energy Fuels* **2005**, *19*, 1879–1888. [[CrossRef](#)]
41. Ewald, J.; Peters, N. A level set based flamelet model for the prediction of combustion in spark ignition engines. In Proceedings of the 15th International Multidimensional Engine Modeling User’s Group Meeting, Detroit, MI, USA, 13 April 2005.

42. Senecal, P.K.; Pomraning, E.; Richards, K.J.; Briggs, T.E.; Choi, C.Y.; McDavid, R.M.; Patterson, M.A. Multi-dimensional modeling of direct-injection diesel spray liquid length and flame lift-off length using CFD and parallel detailed chemistry. *SAE Trans.* **2003**, *112*, 1331–1351.
43. Heywood, J.B. Combustion engine fundamentals. *1ª Edição. Estados Unidos* **1988**, *25*, 1117–1128.
44. Chang, W.; Wang, C.; Wu, Y.; Jin, C.; Zhang, Z.; Liu, H. Study on the mechanism of influence of cetane improver on methanol ignition. *Fuel* **2023**, *354*, 129383. [[CrossRef](#)]

**Disclaimer/Publisher’s Note:** The statements, opinions and data contained in all publications are solely those of the individual author(s) and contributor(s) and not of MDPI and/or the editor(s). MDPI and/or the editor(s) disclaim responsibility for any injury to people or property resulting from any ideas, methods, instructions or products referred to in the content.